Acta Mech 229, 697–705 (2018)
https://doi.org/10.1007/s00707-017-1993-2

ORIGINAL PAPER

S. Casciati · L. Faravelli · M. Vece

Long-time storage effects on shape memory alloy wires

This paper is dedicated to the memory of Franz Ziegler

Received: 1 March 2017 / Revised: 23 May 2017 / Published online: 17 November 2017

Abstract A rich literature studies shape memory alloy (SMA) wires for their potential use in dampers devices able to reduce wind, rain, and traffic-induced oscillations of stayed cables. Restrainers for bridges and improved aseismic devices also exploit alloy components. Thus, SMAs should be regarded as materials susceptible to storage in the yard. In this paper, the authors discuss the evolution of SMA macroscopic behavior as caused by a long-time storage of the product as acquired. The study discriminates between wires of different diameters, because the flat cycles shown by thin wires (i.e., diameter ≤ 0.5 mm) and the non-classical S-shaped cycles of thick wires (of diameter 2.46 mm in this paper) answer differently to environmental modifications. The hysteretic behavior of some specimens of wires, of diameter 2.46 mm, is here investigated to mark the unpredictability of the consequence of a long-time storage, which could prevent from the practical exploitation of such alloys in civil engineering.

1 Introduction

The protection of civil engineering infrastructures is often pursued by adding external devices [1]. Shape memory alloys (SMAs) [2–4] are smart materials with a wide range of practical and potential applications. Some applications were devoted to health solutions, i.e., in orthopedic and orthodontic applications. Their use was also studied for exploitations in dampers for civil engineering [5–9], as well as for their potential in morphing [10]. Review papers [11–13] are available.

The martensitic phase transition (MT) is the key issue in SMA response. This is considered a first-order transition with hysteresis between metastable solid phases. The alloy composition and the heat treatments characterize the transformation behavior [14,15]. The experimental analysis of SMA shows a hysteretic behavior in both stress–strain or strain-temperature representations. Moreover, series of continuous loading–unloading cycles in stress–strain show a monotonic SMA creep and a practical reduction of the available deformation [16–21].

This paper is targeted to the SMA use in dampers devices for civil engineering applications. The different behavior that appears using thin or thick wires of NiTi SMA is first discussed to emphasize the focus on wires

S. Casciati
DICAr, School of Architecture, University of Catania at Siracusa, P.za Federico di Svevia, 96100 Siracusa, Italy

L. Faravelli (✉)
DICAr, University of Pavia, Via Ferrata 3, 27100 Pavia, Italy
E-mail: lucia@dipmec.unipv.it

M. Vece
R2M solution s.r.l., via Fratelli Curzio 42, 27100 Pavia, Italy

of diameters 2.46 mm. The effects of a long-time storage of the material, when forged in wires of this diameter, are then investigated to understand the potential drawbacks of this material in bridge applications.

2 Response of SMA wire specimens to loading–unloading cycles

2.1 Expected qualitative phenomena

Shape memory alloys are different each from the other for ingredients and for percent of each ingredient. The authors only consider NiTi alloys along this paper.

The technological process can affect the specimen properties. Thus, only SMA wires are studied. In particular, reference is made to alloys that behave in the austenite phase at ambient temperature.

As outlined in [22], low-diameter (below 0.5 mm) wires behave differently from wires of larger diameter when a specimen undergoes repeated cycles of loading and unloading.

With reference to Fig. 1a, which holds for small diameter wires, the following quantities characterize the response in the stress (σ)/strain (ε) plane:

- ε_F denotes the maximum strain achieved during each cycle; its value is assigned and drives the standard span-driven test;
- $\varepsilon_{S,i}$ denotes the final strain at the end of the i-th cycle. Its value characterizes the response;
- $\sigma_{t,i}$ denotes the stress value of the nearly flat branch in loading for the i-th cycle;
- $\sigma_{b,i}$ denotes the stress value of the nearly flat branch during the unloading for the i-th cycle.

The last two quantities show deteriorating values as the loading–unloading proceeds. This also occurs to the stress value $\sigma_{F,i}$ achieved when the strain is maximum along each single cycle.

Figure 1b provides a sketch of the response of a wire of larger diameter (say 2.46 mm for the cases reported along this paper).

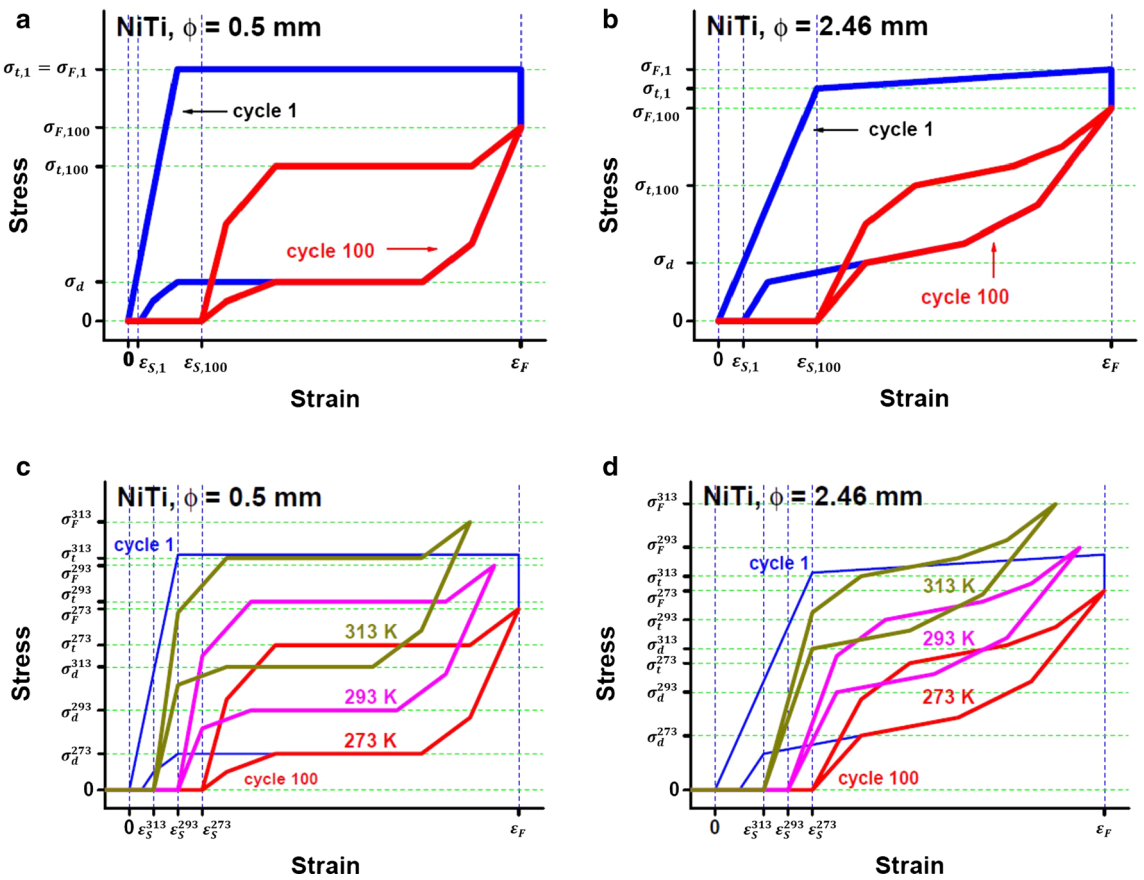

Fig. 1 Expected hysteresis cycles at the beginning and at the end of the training: **a**–**c** wires of small diameter; **b**–**d** wires of larger diameter

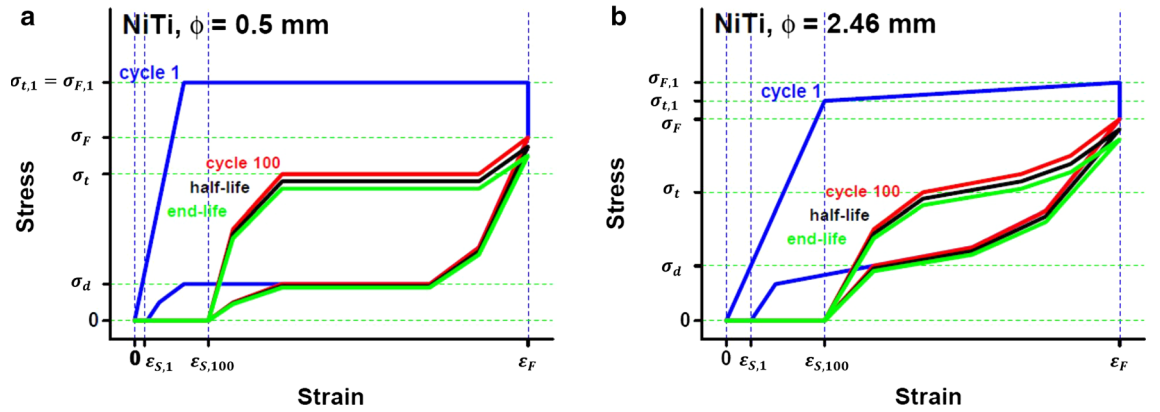

Fig. 2 Expected hysteresis stabilization after the training: **a** wires of small diameter; **b** wires of larger diameter

Two further variables are implicit in the plots: the temperature T (see Fig. 1c, d) and the time t. The latter one is alternatively specified by the number of cycles per second ω or its related frequency $f\,(=\omega/2\pi)$, which is the inverse of the cycle duration d.

The variability of $\varepsilon_{S,i}$ suggests to start any test (or to anticipate any application) by a training consisting of repeated loading–unloading cycles. In this paper, one considers a training of 100 cycles. During the training, the response shows hysteresis of contracting shape. If one proceeds in the test the response stabilizes, as sketched in Fig. 2, until the fatigue lifetime is reached and the hysteresis deteriorates toward failure.

The difference between the top stress and the bottom stress depends on the actual maximum elongation along the cycle. The top stress value depends on the temperature T by the relationship

$$\frac{\mathrm{d}\sigma}{\mathrm{d}T} = CCC, \tag{1}$$

the Clausius–Clapeyron coefficient (i.e., CCC) being in the range from 3 to 20 MPa $^{\circ}\mathrm{C}^{-1}$ for NiTi alloys. One can regard this phenomenon as a shift upward of the strain axis with the temperature.

In Ref. [22], an average value of 6 is assumed for the C–C coefficient. This means a shift up of 120 MPa of the baseline when the temperature decreases from the laboratory value (293 K) to 0°C (i.e., 273 K). For a maximum strain value of 8%, this temperature reduction sees the unloading flat branch of Fig. 1a under the baseline, i.e., the recovering is prevented and the unloading stop with the alloy still in martensite showing a significant residual strain.

When the attention is focused on a wire of larger diameter (Fig. 1b), after the training the hysteresis reaches an S-shaped format that is no longer constrained to low stress values. Thus, a temperature increase would reduce the hysteresis area but it will not be fully lost.

In summary, thinner wires that work by flat cycles remain in martensite when the external temperature is under 273 K. The thick wires, which follow the S-shaped cycles, works satisfactorily between 240 and 340 K [22].

To characterize each cycle along the response, it is useful to introduce the dissipated energy

$$E = V \oint \sigma \, \mathrm{d}\varepsilon \tag{2}$$

with V denoting the specimen volume.

2.2 Laboratory facility

The experimental activity reported in this paper was carried out on an MTS 858 Mini Bionix II (Fig. 3a) universal testing machine, situated in a protected room inside a big conditioned laboratory where the working temperature is around 293 K.

Special attention was devoted to the way the specimen is inserted in the grips (Fig. 3b). Actually, both its ends are inserted in devices made by two plates assembled by four screws. Each couple of plates shows

Fig. 3 Equipment (**a**) and grip detail (**b**)

Table 1 Creep effects after training for NiTi wires of diameter ϕ, initial length l_u, and cycling frequency f

Sample	ϕ (mm)	Effective length (mm)	Cycling frequency (Hz)	Creep effects (mm)
A	2.46	502	0.005	6.80
B	0.50	175	0.05	1.47
C	0.20	163	0.1	1.26

two lateral cylindrical expansions to be mounted (hinged) in a fork whose cylindrical support is gripped to the machine contrasting terminals. In this way, the specimen undergoes the desired tension, but is prevented from any accidental compression [22].

2.3 Material specimens

The material specimens for the authors' laboratory activity were acquired from market providers: in the period from 2007 to 2015 by Memry (CT, USA), a division of SAES Getters (Italy), and previously by Special Metals Corp (NY, USA). All the specimens are made by NiTi alloy in the pseudo-elastic state. The experimental study was focused on the NiTi alloy for two main reasons: its resistance to wet oxidation and the actual offer to the customer of wires of significant length.

The study whose results are reported in the next section used three types of wires of different diameter (Table 1). All of them come from a lot of recent acquisition. The results achieved during experimental campaigns on several specimens, obtained from this lot, are all consistent with those presented here just to confirm the expected behavior depicted in Sect. 2.1. It is worth noting that the surface of the samples of diameter 2.46 mm is finished in a light-gray oxide surface. The other wires come with the surface in black oxide. The austenite start temperatures (A_s) are similar for the two samples (i.e., 248/247 and 243 K, respectively). The supplier certificate indicated that the nominal wire composition was 55.95 and 55.92 wt% of Ni balance Ti, but it includes also minimal quantities (< 0.01 wt%) of more than 25 elements (Si, Cr, Co, Mo, W, Nb, Al, Ba, H, Fe).

Excerpts of wires of type C, acquired for some previous experimental campaigns carried out in the last 2 years, were left in the laboratory depository. All of them remained stored for a duration ranging from 10 to 14 months. The response of specimens obtained from these excerpts is investigated and reported in Sect. 4.

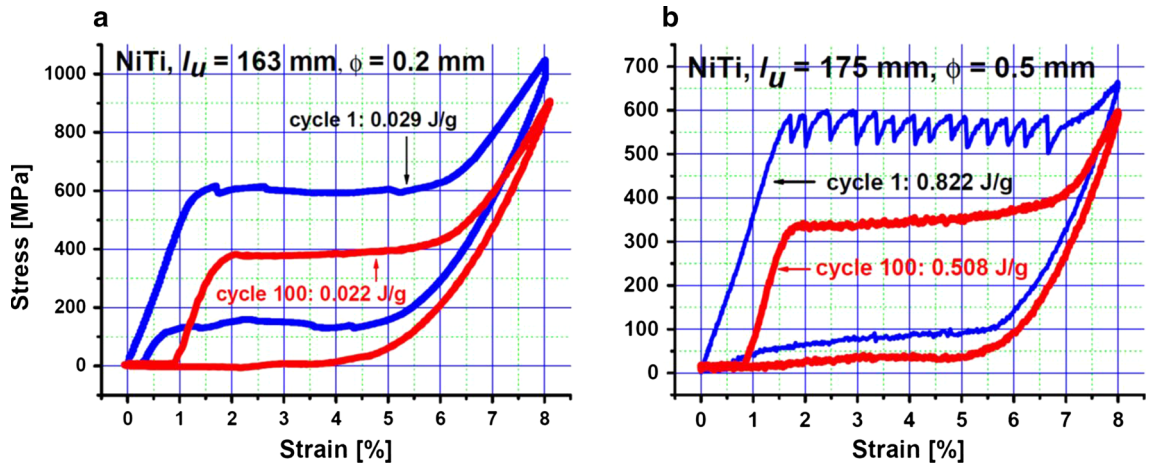

Fig. 4 Cycles 1 and 100 for thin NiTi wires: **a** diameter 0.2 mm and **b** diameter 0.5 mm

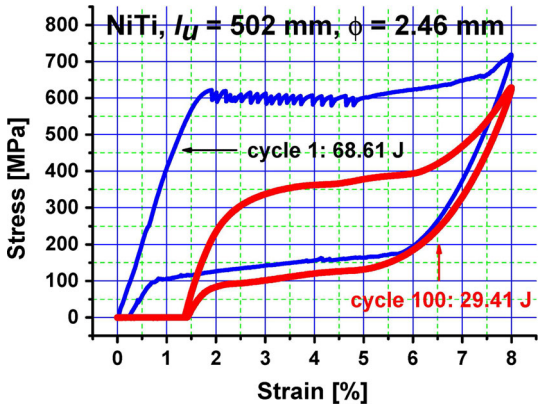

Fig. 5 Cycles 1 and 100 for the NiTi wire of diameter 2.46 mm

3 Training specimens of different diameter as acquired

As specified in Table 1, the three specimens have different initial length and were trained at different cycling frequencies. The residual elongation after the training is reported in the last column of Table 1.

Indeed, the training usually uses 100 sinusoidal cycles up to 8% of deformation at given cycle frequency. The increase in length of the specimen is associated with the maximum stress value (i.e., near 600 MPa) and with their cycling rate. An increase in the external temperature increases the maximum stress and the accumulated deformation, labeled as SMA creep. Increasing the cycling rate, the specimen temperature increases under the action of the dissipation associated to hysteresis, and, subsequently, the SMA creep increases. For larger specimen diameters, the cycling rate has to be reduced proportionally to the radius value. Actually, it is well known that the strong thermomechanical coupling, which characterizes these alloys, leads to a different behavior for different loading rates. Here the authors have chosen a frequency proportional to the inverse of the wire radius. Torra and co-workers [15,22] introduced the reasoning on the back of this choice. The heat content in a cylindrical wire is proportional to the squared value of the section radius, while the output flow is proportional to the radius value. Thus, the net ratio is proportional to the radius. Working with "cylinders" of different diameters, the appropriate cycling frequency increases as the radius decreases. Table 1 shows the cycling rate adopted for the A, B, and C specimens.

The graphical representations of the 1st and 100th cycles are given in Fig. 4 for the thin wires and in Fig. 5 for the sample of diameter 2.46 mm. The figures also show the estimates for the dissipated energy as defined in Eq. (2), but its value is divided by the specimen weight. Different cycling frequencies were selected in the three tests, and this is translated in the higher noise, for lower cycling frequency, as the transformation from austenite to martensite progresses.

Table 2 Creep effects after training for NiTi wires (diameter of 2.46 mm and cycling frequency of 0.01 Hz) that have been stored for 1 year in the laboratory

Id sample	Effective length (mm)	Creep effects (mm)	Creep effects (%)
01	144	1.79	1.24
02	140	2.80	2.00
03	140	8.83	6.31
04	111	4.12	3.71
05	90	2.62	2.91
06	90	2.96	3.29
07	90	2.02	2.24
08	90	3.11	3.46

Table 3 Dissipated energy before and after training for NiTi wires (diameter of 2.46 mm and cycling frequency of 0.01 Hz) that have been stored for 1 year in the laboratory

Id sample	Effective length (mm)	Dissipated energy $_{\text{cycle1}}$ (J/g)	Dissipated energy$_{\text{cycle100}}$ (J/g)
01	144	0.171	0.041
02	140	0.188	0.028
03	140	0.292	0.003
04	111	0.276	0.018
05	90	0.250	0.046
06	90	0.245	0.030
07	90	0.226	0.031
08	90	0.243	0.027

After several cycles of loading–unloading, the stress-induced transformation stress, in "A" and "B" wires, was approximately 350 MPa, i.e., the transformation forces were 1700 N and 70 N, respectively.

Figure 4 confirms the remark of Sect. 2.1. In the tested specimens, even a decrease in temperature of a few degrees would prevent the regular ending of the cycle. As a general conclusion when using SMA to design a damper, the adoption of wires of diameters resulting with an S-shaped hysteresis after the training should be preferred. They are more difficult to store than the thin diameters wires, easily coiled on sprockets. The next section is devoted to specimens of diameter 2.46 mm.

The previous way to distinguish between specimens of the types A and B from the C ones could also have been introduced on the basis of grain size and grains orientation. Previous investigations by the authors and associates [15,21,22] pointed out the multigrain character of the acquired samples of diameter 2.46 mm. Nevertheless, specimens obtained from different lots, tested as acquired, always showed similar pseudo-elastic cycles, consistent with Fig. 5, even if with minor differences in the achieved residual creep.

4 Specimens trained after a relatively long storage period

The hysteretic behavior, outlined in previous sections, is affected by several external factors. The specimens of Table 2 were available and were trained according to the same policy illustrated in Sect. 2. These specimens were acquired and stored in the basement rooms of the laboratory for more than 1 year. Several authors in the literature [23–25] mentioned the effects due to the storage at room temperature, which can change the properties of the appropriate alloys. Indeed, time effects are related, for instance, in Cu based to internal changes as the stabilization. In NiTi the stabilization is a minor effect and difficult to be detected [26].

The result of each test is given in Fig. 6 according to the format already adopted in Figs. 4 and 5, namely by reporting the first and the 100th hysteresis cycles. The calculated values of the dissipated energy are summarized in Table 3. All the plots in Fig. 6 confirm that, after hundred cycles, the alloy may not properly recover the strain, and the sample length increases in a way not due to the classic SMA behavior. The long-term storage affects randomly the residual displacement at the end of the first cycle, and this directly influences the shape of the cycle at the end of the training.

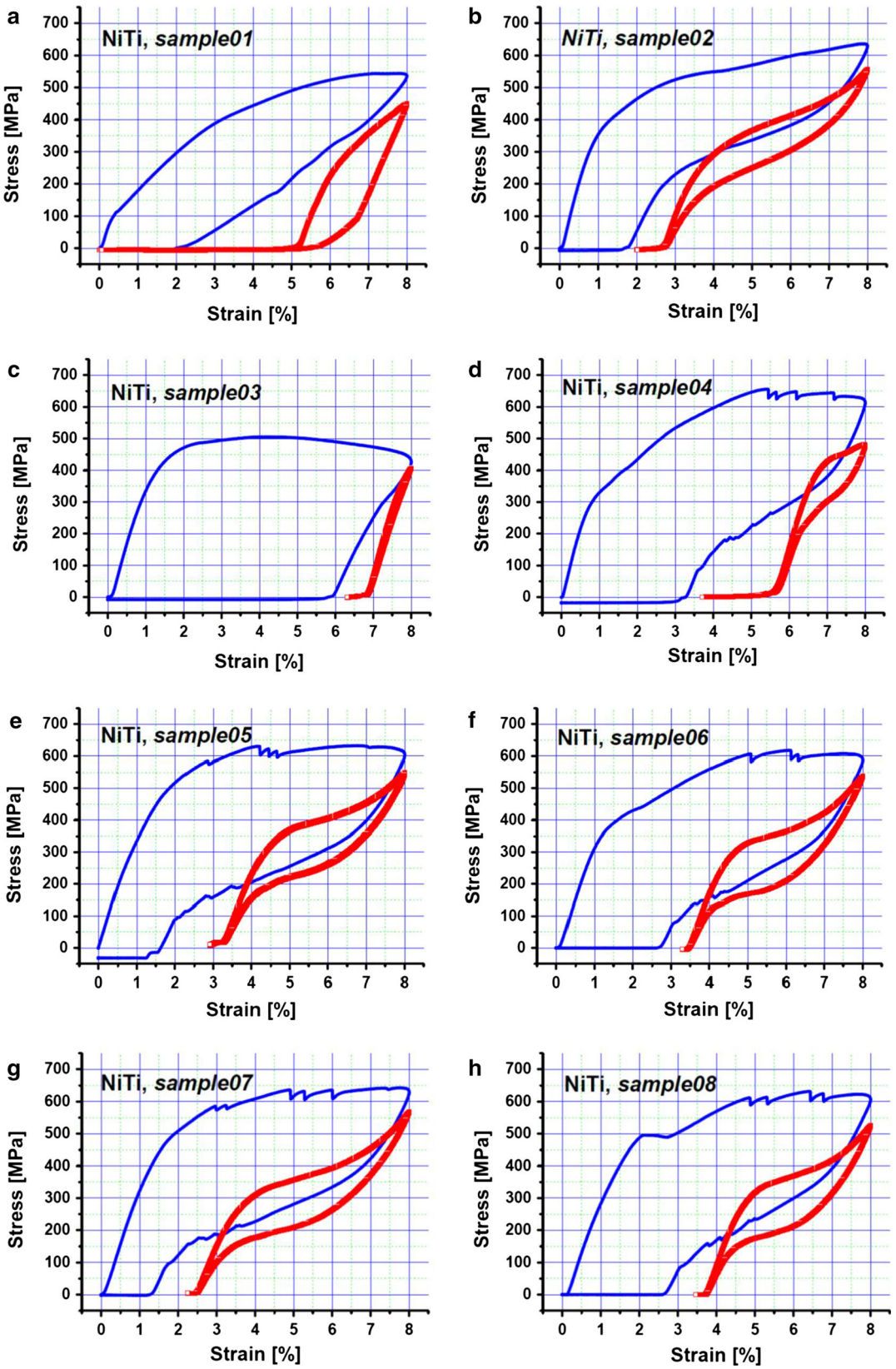

Fig. 6 Training of NiTi wires that underwent the time effect

5 Conclusions

The significant values of the forces encountered in civil engineering applications lead one to adopt either wrapped wires of very small diameter or wires of diameters larger than 1.5 mm. The summer–winter temperature excursions produce effects that are better managed by selecting wires of large diameter.

Unfortunately, it is not easy to arrange thermal treatments for these large diameter wires in the yard. The material has to be stored and then mounted as it is. This paper outlines how the storage period produces a sort of "anomaly" in the hysteretic behavior of the samples. Its main feature is the unpredictability of the effect on the shape of the first cycle, as well as on the left capability of dissipating energy at the material stabilization (i.e., after the training).

As an attempt to justify such situation, one guesses that the procedure of wire preparation by the manufacturer included large deformation hardening. This resulted in that the wires as acquired were actually showing the expected pseudo-elastic behavior. It is then likely that during the successive year aging some softening occurred and the dislocation yield limit decreased. Thus, the samples lost the property of pseudo-elasticity, but recovered it again after 100 cycles of training, in the course of which large irreversible deformation produced new hardening.

Acknowledgements Research Athenaeum Grants (FAR) from both the universities of Catania and Pavia are deeply acknowledged in supporting experiments and mobility. The first author also acknowledges the support by the PRIN2015 grant coordinated at a national level by Prof. M. Di Paola of the University of Palermo.

References

1. Khalid, B., Ziegler, F.: A novel aseismic foundation system for multipurpose asymmetric buildings. Arch. Appl. Mech. **82**, 1423–1437 (2012). https://doi.org/10.1007/s00419-012-0667-8
2. Auricchio, F., Faravelli, L., Magonette, G., et al.: Shape Memory Alloys: Advances in Modelling and Applications. CIMNE, Barcelona, Spain (2001)
3. Lexcellent, C.: Shape-Memory Alloys Handbook. Wiley-ISTE, New York (2013)
4. Lecce, L., Concilio, A.: Shape Memory Alloy Engineering: For Aerospace, Structural and Biomedical Applications. Elsevier, Amsterdam (2014)
5. Casciati, S., Faravelli, L.: Structural components in shape memory alloy for localized energy dissipation. Comput. Struct. **86**, 330–339 (2008)
6. Casciati, F., Faravelli, L., Fuggini, C.: Cable vibration mitigation by added SMA wires. Acta Mech. **195**(1–4), 141–155 (2008)
7. Casciati, F., Faravelli, L.: A passive control device with SMA components: from the prototype to the model. Struct. Control Health Monit. **16**(7–8), 751–765 (2009)
8. Carreras, G., Casciati, F., Casciati, S., et al.: Fatigue laboratory tests toward the design of SMA portico braces. Smart Struct. Syst. **7**(1), 41–57 (2011)
9. Carreras, G., Casciati, S., Terriault, P., et al.: On the NiTi wires in dampers for stayed cables. Smart Struct. Syst. **13**(3), 353–374 (2014)
10. Barbarino, S., Saavedra Flores, E.I., Ajaj, R.M., et al.: A review on shape memory alloys with applications to morphing aircraft. Smart Mater. Struct. **23**(6), 1–19 (2014)
11. Saadat, S., Salichs, J., Noori, M., et al.: An overview of vibration and seismic applications of NiTi shape memory alloy. Smart Mater. Struct. **11**, 218–229 (2002)
12. Song, G., Maa, N., Li, H.N.: Applications of shape memory alloys in civil structures. Eng. Struct. **28**, 1266–1274 (2006)
13. Ozbulut, O.E., Hurlebaus, S., DesRoches, S.: Seismic response control using shape memory alloys: a review. J. Intell. Mater. Syst. Struct. **22**(14), 1531–1549 (2011)
14. Lovey, F.C., Torra, V.: Shape memory in Cu-based alloys: phenomenological behavior at the mesoscale level and interaction of martensitic transformation with structural defects in Cu-Zn-Al. Prog. Mater. Sci. **44**(3), 189–289 (1999)
15. Torra, V., Isalgue, A., Lovey, F.C., et al.: Shape memory alloys as an effective tool to damp oscillations. Study of the fundamental parameters required to guarantee technological applications. J. Therm. Anal. Calorim. **119**(3), 1475–1533 (2015)
16. Casciati, F., Casciati, S., Faravelli, L.: Fatigue characterization of a Cu-based shape memory alloy. Proc. Estonian Acad. Sci. Phys. **56**(29), 207–217 (2007)
17. Casciati, S., Marzi, A.: Experimental studies on the fatigue life of shape memory alloy bars. Smart Struct. Syst. **6**(1), 73–85 (2010)
18. Faravelli, L., Marzi, A.: Coupling shape-memory alloy and embedded informatics toward a metallic self-healing material. Smart Mater. Syst. **6**(9), 1041–1056 (2010)
19. Casciati, S., Marzi, A.: Fatigue tests on SMA bars in span control. Eng. Struct. **33**(4), 1232–1239 (2011)
20. Casciati, F., Casciati, S., Faravelli, L.: Fatigue damage accumulation in a Cu-based shape memory alloy: preliminary investigation. CMC Comput. Mater. Continua **23**(3), 287–306 (2011)
21. Casciati, S., Faravelli, L., Vece, M.: Investigation on the fatigue performance of Ni–Ti thin wires. Struct. Control Health Monit. **24**(1), Article Number: UNSP e1855 (2017)

22. Torra, V., Casciati, S., Vece, M.: Shape memory alloys wires: from small to medium diameter. In: Proceedings of CIMTEC 2016, 5th International Conference on Smart and Multifunctional Materials, Structures and Systems, Perugia, Italy (2016)
23. Kustov, S., Pons, J., Cesari, E., et al.: Two-stage reverse transformation in hyperstabilized β_1' martensite. Scripta Mater. **46**, 817–22 (2002)
24. Kustov, S., Pons, J., Cesari, E., et al.: Stabilization and hyperstabilization of Cu–Al–Be β_1' martensite by thermal treatment and plastic deformation. Mater. Sci. Eng. A **378**, 283–288 (2004)
25. Sapozhnikov, K., Golyandin, S., Kustov, S., et al.: Defect assisted diffusion and kinetic stabilization in Cu–Al–Be β_1' martensite. Mater. Sci. Eng. A **481–482**, 532–537 (2008)
26. Torra, V.: Personal Communication (2017)